Available online at www.sciencedirect.com
SCIENCE DIRECT®
Journal of Power Sources 142 (2005) 264–278
JOURNAL OF POWER SOURCES
www.elsevier.com/locate/jpowsour

Reliability modeling and assessment of grid-connected PEM fuel cell power plants

M. Tanrioven*, M.S. Alam

Department of Electrical and Computer Engineering, University of South Alabama, Mobile, AL 36695-0002, USA

Received 29 September 2004; accepted 25 October 2004
Available online 30 December 2004

Abstract

Fuel cell (FC) power plants are subject to a number of possible outage and derated states due to partial or full failure of auxiliaries. Furthermore, most of the power system reliability studies reported in the literature assume mean values of the particular measure of reliability. However, the reliability indices for grids such as failure rate, outage duration, etc. vary for different time period due to weather conditions, variety of power demands and random faults. It is essential to obtain the estimation of reliability under all environmental, operational and loading conditions. This paper considers above mentioned seasonal variation of grid reliability indices as well as partial or full failure of fuel cell auxiliaries for grid-connected PEM fuel cell power plants (FCPPs). In the paper, a detailed state–space model of the grid-connected FCPP is presented which is a combination of proton exchange membrane fuel cell (PEMFC) power plant generation model and grid outage model. The state–space generation model of a PEMFC power plant is formed based on the failure modes of system auxiliary components. As for the grid outage state–space modeling, the effects of weather conditions such as normal and adverse weather are taken into consideration in modeling the failure and repair rates. The functional relationship between weather conditions and transition rates, namely failure and repair rates are developed based on the fuzzy set theory and embedded into Markov model (MM). Simulation results are obtained for a 5 kW grid-connected PEMFC that supplies a typical residential house using the MATLAB software package.

Keywords: Reliability; Markov model; Fuel cell power plant

1. Introduction

The main objective of any utility in the new competitive environment would be to supply customers with electrical energy as economically as possible with a higher degree of reliability and quality. Electric utility companies have been making every effort to achieve this objective in many ways, one of which is to widen distributed generation (DG) usage. Among the various types of DGs, fuel cells (FC), particularly proton exchange fuel cells (PEMFCs), generated tremendous interest for electricity and heat generation due to its low operating temperature, fast start up characteristics and ecological cleanness [1].

Studies that quantify power system reliability have so far been limited to constant transmission rates, covering two weather conditions, namely normal and adverse weather [2,3]. In reality, however, the probability of a system or a component failure varies from time to time dependent upon factors such as a change of environmental conditions, demand variation and random failures in the system. For better system operation and to aid the formulation of investment policy, the variation of reliability under different weather conditions should be known. Identifying the system reliability variations for different conditions is crucial for fuel

* Corresponding author. Tel.: +1 251 460 7484.
E-mail address: mtanrioven@usouthal.edu (M. Tanrioven).

0378-7753/$ – see front matter © 2004 Elsevier B.V. All rights reserved.
doi:10.1016/j.jpowsour.2004.10.030

cell systems since it is an emerging area of technology. To increase competitiveness and market value of the FCPP, it is important to analyze FC System Reliability for possible environmental, operational and loading conditions. Although numerous studies have been performed in the field of power system reliability, to the best of the authors knowledge, no work has been reported in the area of FC system reliability, possibly due to the early stage of FC technology development and unavailability of sufficient data. This paper develops a grid-connected FC system reliability analytical model based on MM for multiple weather conditions of the grid and state of health of the FC system. The proposed model includes a detailed state–space generation model for FCPP and a state–space Markov model (MM) for grid outage. Fuzzy set theory is used in the MM that is called fuzzy Markov model (FMM), to incorporate both transition rates and temperature-based seasons, which include multiple weather conditions such as normal, less stormy and very stormy.

2. Overview

2.1. Generation unit reliability

Most generation units requires a number of auxiliary equipment and therefore they are subject to different possible derated capacity states based on the factors such as outages of auxiliaries, fuel quality and environmental conditions [4]. Hence, the state–space model of generating unit is not limited to just possible two conditions of 1 and 0, but can have different states such as operation, derated, fully faulted or maintenance. For instance, a thermal power plant has auxiliary components such as water pumps, cooling fans, boiler and turbine. Each of the auxiliary failure may produce many partial outages, which results in either derated or outage states.

The number of outage state is given by $2^n - 1$ in Markov processes, where n is the number of elements that affect the system's state of health. However, the probability of more than one auxiliary component failure at the same time is extremely rare and therefore such states can be neglected.

The general state–space model of a generating unit for the aforementioned case is given in Fig. 1, where λ represents failure rate, μ represents repair rate, indices $i = 1, 2, \ldots, k$ represent the number of components that cause unit failure, and $j = 1, 2, \ldots, m$ represent the number of components that affect derating level of the unit. In various cases, some other factors such as climate conditions and poor-quality fuel may cause derated states for generating units. For instance, fuel quality is vitally important for FCPP in order to operate them economically and efficiently.

2.2. Continuous Markov model

In the field of reliability assessment, Markov processes use state transition rates [5]. State transitions in Markov processes occur continuously rather than at discrete time intervals and both system states and transition rates together constitute state–space diagram. Hence, Markov processes can be easily applied to power system reliability since failure rates are equivalent to state transition rates. The general structure of a continuous-time, discrete state equation for a

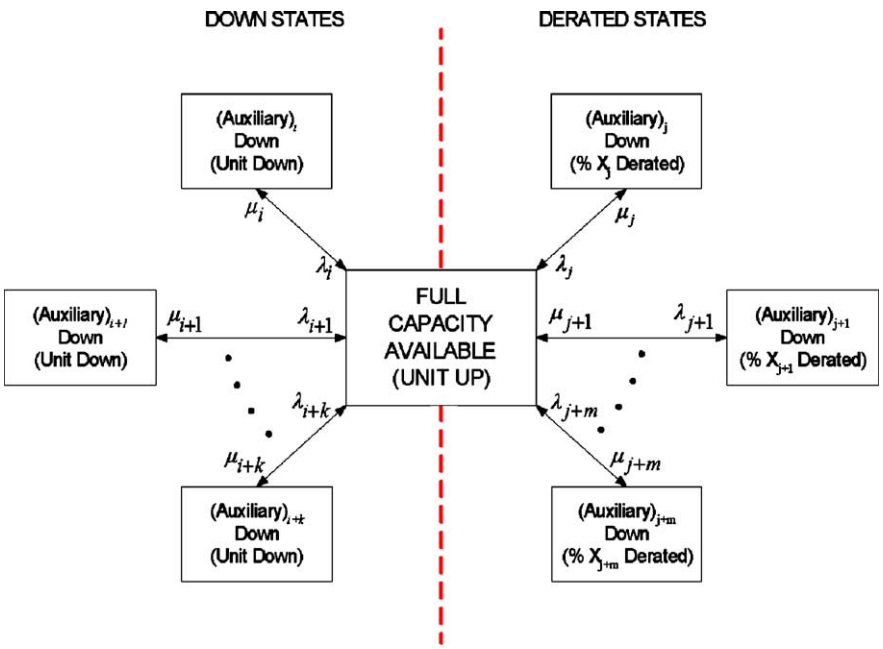

Fig. 1. The state–space model of the generating unit.

MM with n states can be described as [6]:

$$\frac{\mathrm{d}}{\mathrm{d}t}\begin{bmatrix} P_1(t) \\ P_2(t) \\ \vdots \\ P_n(t) \end{bmatrix} = \begin{bmatrix} -\sum_{i=2}^{n} \lambda_{1i} & \lambda_{21} & \cdots & \lambda_{n1} \\ \lambda_{12} & -\sum_{i=1,i\neq 2}^{n} \lambda_{2i} & \cdots & \lambda_{n2} \\ \vdots & \vdots & \vdots & \vdots \\ \lambda_{1n} & \lambda_{2n} & \cdots & -\sum_{i=1}^{n-1} \lambda_{ni} \end{bmatrix} \cdot \begin{bmatrix} P_1(t) \\ P_2(t) \\ \vdots \\ P_n(t) \end{bmatrix} \quad (1)$$

Eq. (1) can be rewritten as

$$\frac{\mathrm{d}}{\mathrm{d}t} P_i(t) = A \cdot P_i(t) \quad (2)$$

where λ_{ij} represents the transition rate between the ith and jth states, $p_i(t)$ represents the probability of ith state, and A represents the transition matrix. In the conventional Markov model (CMM), the transition rates, λ_{ij}, are constant valued and the states have two possible conditions—1 and 0. While the summation of the probabilities of states with logic 1 gives the availability of the system, the summation of states with logic 0 probabilities gives the unavailability of the system. However, the state–space method is not limited to just two conditions, 1 and 0, but components can have different states such as operation, derated, fully faulted or maintenance [6,7].

3. Proposed method

As for any power system, the reliability of a grid-connected FCPP corresponds to a measure of the extent to which it supplies the load requirement with acceptable continuity and quality. To achieve this goal, power system reliability engineers must incorporate the reliability of all system components under various environmental and operational conditions pertaining to any specified period. Although environmental effects on the system reliability should be taken into consideration for grid supply system, it is negligible for commercially available FCPPs because they are placed at the location of end-users. However, FCPPs are subject to a number of possible outage and derated states due to partial or full failure of auxiliaries [8–10]. Some fuel cell failure modes are such as membranes drying out (insufficient humidification), overheating, passages clogging up with water, and freezing of water in humidification channels. In this paper, methodology in modeling the reliability of FCPP as well as grid reliability model, which takes into account the environmental effects have been developed, and individual reliabilities for FCPP and grid are calculated. Afterwards, the aforementioned two considerations are combined using network representation techniques to evaluate the entire system reliability.

3.1. Development of reliability model for PEMFC

FCPPs basically convert chemical energy of hydrocarbon fuels, typically such as natural gas, into DC form of electrical energy. A FCPP mainly consists of a fuel-processing unit (reformer), FC stack and power conditioning unit. The FC uses hydrogen as input fuel and produces DC power at the output of the stack. A simple representation of a FCPP is shown in Fig. 2.

The performance of the stack is expressed by the polarization curve, which gives the relationship between the stack terminal voltage and load current. In order to ensure FCPP's robustness and adaptation to load variations, the characteristic of polarization curve should be kept at a constant level

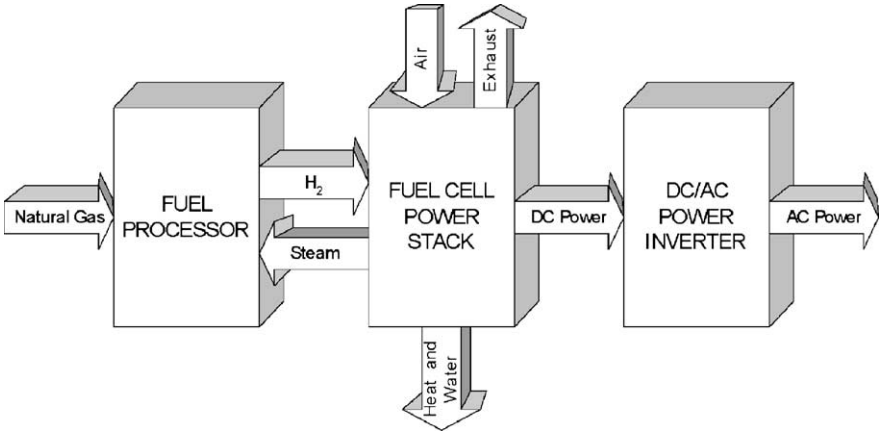

Fig. 2. Basic components of a fuel cell power plant.

by controlling the parameters such as reactant flow rate, total pressure, reactant partial pressure, temperature, and membrane humidity [11]. To control these parameters, various auxiliary components such as blowers for cooling and reactant air, pump for hydrogen circulation and humidifier for reactant air are used in the FCPP system. For power conversion and system control, the power conditioning unit includes a DC/DC converter, a DC/AC inverter, an overall controller, a transformer and auxiliary energy storage devices such as battery and super-capacitor. However, the number and types of auxiliaries may be different for different FCPPs depending on the applications. In this research, a PEM FCPP is considered which includes the auxiliary components along with the input and output signals as shown in Fig. 3.

As shown in Fig. 3, the fuel cell system includes the fuel cell stack, plus all of the auxiliary equipment such as air compressors, pumps, humidification equipment, coolers and control electronics. During normal operation, fuel cell system components such as compressor, fans, pumps, motors, temperature and humidity sensors, relays, and other control electronics could contribute to a system failure or derated mode for different reasons such as ignition of any leaking hydrogen, material fatigues, wear outs, break downs, membrane drying out, overheating, and freezing of water in channels [10]. If any of the components go beyond its operational limit, the corresponding output will be degraded by a factor. For instance, insufficient circulating coolant flow due to the failure of coolant water pump may cause a reduction in the nominal. Other failures may cause either a reduction in nominal output power or total system outage.

3.1.1. Development of state–space model for PEMFC system

The PEM fuel cell DC stack voltage including all irreversibilities may be expressed as [12]

$$V_{\text{stack}} = V_{\text{open}} - V_{\text{ohmic}} - V_{\text{activation}} - V_{\text{concentration}} \tag{3}$$

where

$$V_{open} = N_0 \cdot (E^0 + E^1) = N_0 \cdot \left[-\frac{\Delta \bar{g}_f^0}{2F} + \frac{RT}{2F} \ln \left(\frac{p_{H_2} \cdot \sqrt{p_{O_2}}}{p_{H_2O}} \right) \right] \tag{4}$$

is called the Nernst voltage or reversible voltage that exists at no load condition for a given temperature and pressure,

$$V_{\text{ohmic}} = (i + i_n) \cdot R_{\text{FC}} = I_{\text{dc}} \cdot R_{FC} \tag{5}$$

is the resistive voltage loss due to the resistance of non-ideal electrodes and connections and the resistance to proton flow

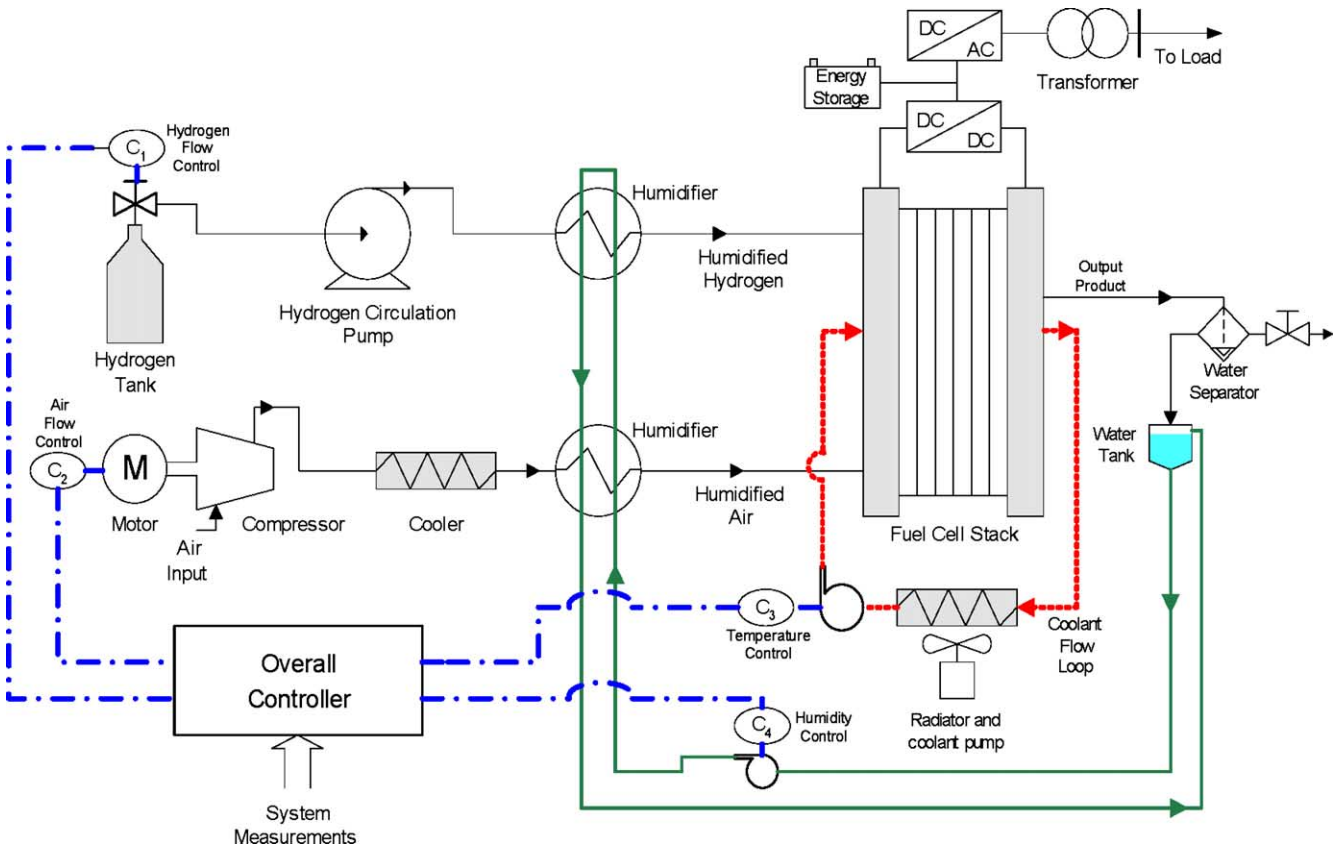

Fig. 3. A PEM fuel cell based FCPP system.

in the PEM,

$$V_{\text{activation}} = N_0 \cdot \frac{RT}{2\alpha F} \cdot \ln\left(\frac{I_{\text{dc}}}{I_0}\right) \quad (6)$$

is the voltage loss corresponding to the activation losses due to the rate of reactions taking place on the surface of the electrodes, and

$$V_{\text{concentration}} = -c \cdot \ln\left(1 - \frac{I_{\text{dc}}}{I_{\text{Lim}}}\right) \quad (7)$$

is the voltage loss corresponding to the voltage change due to mass transport losses, where c is $(RT/2F)$ for PEMFC. The parameters used in the above equations are defined as:

N_0 is the cell number, V_0 the open cell voltage (V), E^0 the cell emf at STP (25 °C and 1 atm) (V), Δg_f^0 the change in Gibbs free energy, R the universal gas constant (8.1345 J mol^{-1} K^{-1}), T the temperature of the fuel cell stack (K), F the Faraday's constant (96485 C mol^{-1}), P_{H_2} the hydrogen partial pressure (atm); $P_{\text{H}_2\text{O}}$ the water partial pressure (atm), P_{O_2} the oxygen partial pressure (atm), α the charge transfer coefficient, I_{dc} the current of the FC stack (A), I_{Lim} the limiting current of FC stack (A), I_0 the exchange current density stack (A cm^{-2}) and c the empirical coefficient.

The total stack power is defined as $P = V_{\text{stack}} \cdot I_{\text{dc}}$.

3.1.2. Cooling system

To operate fuel cells effectively, a coolant fluid must be circulated through the fuel cell. The fundamental components of the coolant flow loop system consist of a coolant pump, a radiator and a fan as shown in Fig. 3. The cooling system adjusts the FC temperature at an efficient operating point. The cooling system includes mechanical and electrical parts such as radiator, fan, motor and motor drives. After a prescribed period of operation, the mechanical parts could experience deformations such as cracks, breakdowns and holes in radiator, pump and fan blades due to fatigue as well as wear-out and stresses, which may result in insufficient cooling. Furthermore, electrical motor and/or electrical drives may malfunction due to failures in control circuit and other related reasons. The same types of failures may also occur for other FC sub-systems that cause a reduction in the FCPP output. The impacts of the aforementioned auxiliary failures are considered herein rather than the failure modes to calculate the reduction in overall FCPP system performance. Assume that there is insufficient cooling due to a reduction in the cooling system performance, which changes the operating temperature of the FCPP by ΔT, and the new operating temperature can be expressed as:

$$\dot{T} = T + \Delta T \quad (8)$$

The increase in temperature leads to a reduction in the FCPP output voltage due to the Gibbs free energy, which is a chemical energy and converted into electrical energy, changes inversely with temperature as shown in the following equation [2].

$$\dot{V}_{\text{stack}} = V_{\text{stack}} - \Delta V \quad (9)$$

In other words, the reversible open circuit voltage for a hydrogen fuel cell, which is given by $V_{\text{open}} = (-\Delta \overline{g}_f/2F)$, will decrease with increasing temperature. The situation can be summarized for the other irreversibilities in Eq. (3) as follows:

- Resistive voltage loss, V_{ohmic} tends to increase at higher temperature due to dry out mode of the fuel cell stack. Because drying of the membrane leads to a poor protonic conductivity of the PEM membrane, which means that an increase in resistive losses is more probable at higher operating temperature,
- Activation voltage loss, $V_{\text{activation}}$ will increase due to the $(RT/2\alpha F)$ factor in Eq. (6). Thus $V_{\text{activation}}$ is directly proportional to temperature T
- The only decrease takes place at concentration voltage loss due to the $-(RT/2F)$ factor in Eq. (7). However, the percentage of voltage reduction in $V_{\text{consentration}}$ is smaller than the percentage voltage increase in $V_{\text{activation}}$ due to the coefficient α that takes a value between zero and one (generally $\alpha = 0.5$). Hence, a decrease in the maximum power level will be observed for higher temperature as shown in Eq. (10), where $\Delta P = \Delta \text{V} \cdot I_{\text{dc}}$.

$$\dot{P} = P - \Delta P \quad (10)$$

Consequently, if the temperature increases due to insufficient cooling, the power supplying capacity of fuel cell decreases, which can be calculated as:

$$\text{RP}_{\text{C}}(\%) = \frac{P - \Delta P}{P} \times 100 = \frac{\dot{P}}{P} \times 100 \quad (11)$$

where RP_{C} is the percent reduction in power supplying capacity of fuel cell due to insufficient cooling. If the FCPP coolant system completely fails or if the failure causes instability in the FCPP operation leading to an emergency shutdown of the system, this phenomenon can be represented by a state–space model as shown in Fig. 4.

3.1.3. Humidification system

Appropriate humidification of the reactant gasses is vital for proper functioning of a PEM fuel cell stack. PEM fuel cells are quite sensitive to the humidity of the reactant gases, and the excess liquid water from the humidification process that flows into the fuel cell can reduce the output power capacity and may cause stack damage. The humidification system is expected to keep relative humidity of the reactants at around 100% level and a maximum temperature of 60 °C, which is achieved by injecting water vapor into the air stream of the humidifier. Büchi and Srinivasan [13] showed that operating a PEM fuel cell without humidification reduces the fuel cell power supplying capacity by 40%. This loss of performance is mainly caused by internal ohmic resistance increase resulted from drying-out of the membrane.

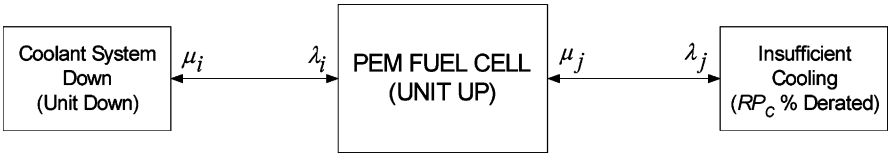

Fig. 4. The effect of cooling system failure on FCPP generation using state–space representation.

The membrane dry-out mode increases the magnitude of the fuel cell stack impedance, expressed as

$$\dot{R}_{\mathrm{FC}} = R_{\mathrm{FC}} + \Delta R \tag{12}$$

The reduction level in FCPP output power depends upon the severity of insufficient humidification. From Eq. (3), it is obvious that the resistive voltage loss, V_{ohmic} is directly proportional to FC stack resistance, which leads to output voltage reduction and consequent power reduction. Since humid reactants are a mixture of dry gasses and vapor, dry partial pressure results due to the difference between total pressure and vapor pressure, expressed as

$$\dot{p}_{\mathrm{T}} = p_{\mathrm{T}} - p_{\mathrm{v}} \tag{13}$$

Since humidity ratio, ϕ is expressed as the ratio of partial pressure of water vapor (P_{v}) to saturation pressure (P_{s}), then the vapor pressure (P_{v}) can be expressed as

$$p_{\mathrm{v}} = \phi \cdot p_{\mathrm{s}} \tag{14}$$

Considering total system pressure (P_{T}) and the factors that contributes to the partial pressure, Eq. (14) can be rewritten as

$$p_{\mathrm{H_2}} = w \cdot p_{\mathrm{T}}, \quad p_{\mathrm{O_2}} = x \cdot p_{\mathrm{T}}, \quad p_{\mathrm{H_2O}} = y \cdot p_{\mathrm{T}} \tag{15}$$

where w, x and y are constants related to molar masses and concentrations of H_2, O_2 and H_2O, respectively. Substituting Eq. (14) into Nernst voltage, Eq. (4) rewritten as

$$V_{\mathrm{open}} = E^0 + \frac{RT}{2F} \cdot \ln\left(\frac{w \cdot \sqrt{x}}{y}\right) + \frac{RT}{4F} \ln(p_{\mathrm{T}}) \tag{16}$$

From Eqs. (13) and (16), it is evident that if the total system pressure, P_{T}, is reduced to $\dot{p}_{\mathrm{T}}$, then the open circuit voltage and the corresponding output voltage will be reduced by $\frac{RT}{4F} \ln(p_{\mathrm{T}} - \dot{p}_{\mathrm{T}})$.

Assume that $\mathrm{RP_H}$ represents the percent reduction in power supplying capacity of the FCPP due to insufficient humidification. Then the state–space model of this event can be represented as shown in Fig. 5. It may be mentioned that possible stack failure due to lack of humidification is not considered in the model.

3.1.4. Fuelling system

In a PEM fuel cell, continuous flow of hydrogen must be maintained to ensure seamless electrical energy output. Various types of hydrogen supply system are possible depending on factors such as hydrogen production, fuel cell size, and hydrogen storage. The simplest system is to use high-pressure tank, where the hydrogen flow rate is controlled through a valve. Another possible way for performing the hydrogen circulation is to use hydrogen-circulating pump. The objective of the hydrogen flow control is to homogenize the pressure throughout the stack. As well as some mechanical wear outs and control malfunction, degeneration of pure hydrogen may be the cause of any possible reduction in state of health of hydrogen supply that leads to derated states of FC unit.

For the fuel cell generation model, assume that there is an insufficient hydrogen supply to the FC input. Since $Q = 2F \times w_{\mathrm{H_2}} = I_{\mathrm{dc}} \times t$ is the charge and $w_{\mathrm{H_2}}$ is the amount of hydrogen in mol, then

$$I_{\mathrm{dc}} = 2F \times \frac{w_{\mathrm{H_2}}}{t} = 2F \times q_{\mathrm{H_2}} \tag{17}$$

where $q_{\mathrm{H_2}} = (w_{\mathrm{H_2}}/t)$, I_{dc} is the total stack current, and $q_{\mathrm{H_2}}$ the molar hydrogen usage per second. If stack current is written in terms of total stack power, then $I_{\mathrm{dc}} = P/V_{\mathrm{stack}}$. Eq. (17) can thus be rewritten as

$$P = 2F \cdot q_{\mathrm{H_2}} \cdot V_{\mathrm{stack}} \tag{18}$$

If there is a reduction in maximum designed level of hydrogen usage reduces by $\Delta q_{\mathrm{H_2}}$ for any of the hydrogen circulating system, then the corresponding decrease in the FCPP output power can be expressed as

$$\Delta P = 2F \cdot \Delta q_{\mathrm{H_2}} \cdot V_{\mathrm{stack}} \tag{19}$$

Thus, the percent reduction in power supplying capacity of FCPP due to insufficient hydrogen usage can be calculated as

$$\mathrm{RP_q}(\%) = \frac{q_{\mathrm{H_2}} - \Delta q_{\mathrm{H_2}}}{q_{\mathrm{H_2}}} \times 100 = \frac{\dot{q}_{\mathrm{H_2}}}{q_{\mathrm{H_2}}} \times 100 \tag{20}$$

The state–space model shown in Fig. 6 illustrates the effect of hydrogen supply system failure on FCPP power generation.

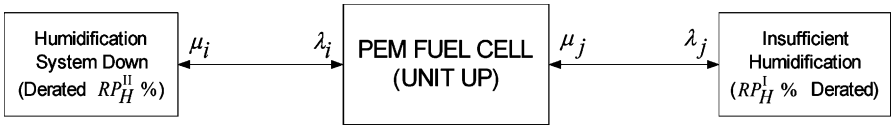

Fig. 5. The effect of humidification system failure on FC generation in terms of state–space representation.

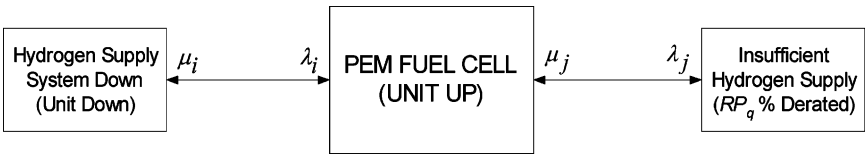

Fig. 6. The effect of hydrogen supply system failure on FCPP power generation in terms of state–space representation.

3.1.5. Air circulating system

The oxygen derived from air is used to complete the reaction in a FCPP. The air flow is controlled by regulating the input voltage of the compressor motor in order to maintain desired amount of oxygen. The molar oxygen usage of the FC per second, q_{O_2} for a given output power can be computed as

$$q_{O_2} = \frac{P}{4FV_{\text{stack}}} \tag{21}$$

Eq. (15) can be adopted to calculate air usage by multiplying q_{O_2} with 0.21 since 21% oxygen is available in the air mixture. However, in real applications the blower and compressor are sized such that the excess oxygen ratio γ is equal to 2 [14], given by

$$\gamma = \frac{\text{supplied rate of } O_2}{\text{reacted rate of } O_2} \tag{22}$$

For modeling FCPP system generation, assume that the air supply is insufficient due to factors such as possible partial failures and wear outs. Since abundant oxygen is supplied, FCPP output will not be affected unless partial pressure of oxygen drops below the critical level, which may lead to catastrophic membrane failure. An emergency stop function will either isolate the system from load or shut down the system. Thus possible failure in air flow system either reduces or leads to total air circulation outage. The failure modes in air flow circulation do not lead to any derated state but results in FCPP system failure. The state–space model in Fig. 7 demonstrates the effect of oxygen supply system failure on FCPP based power generation.

3.1.6. Energy storage system

The hydrogen flow rate is controlled continuously in order to follow the electrical load variations. However, depending upon the FCPP system type, this flow rate adjustment can be achieved with a time delay, ranging from a few microseconds to 30 s. Therefore, some type of energy storage is needed for fast transient response to meet the peak load requirement. Among the various energy storage devices, batteries are the common choice, and they have relatively shorter lifetime and need periodic maintenance. Although energy storage selection is a complex process and needs to satisfy a number of criteria, our objective here is to maintain the power supply at the needed level. If the FCPP output power is P and system peak load is P_{peak}, then based on 80% battery usage, the required energy storage power is given by

$$P_{\text{storage}} = 1.25 \times (P_{\text{peak}} - P) \tag{23}$$

The energy storage capacity is measured as $W = P_{\text{storage}} \times t$, where t is the number of hours used for supplying the power, P_{storage}. To evaluate the effects of energy storage on FCPP reliability, several factors such as maintenance, energy storage lifetime, and mean time between failures (MTBF) should be used. If the total power supply capacity of the system falls below the load demand due to energy storage performance loss and/or failures, the excess load can no longer be supplied and must be disconnected from the system by using a smart energy management control system. The percent reduction in the FCPP power supply capacity due to energy storage failure may be calculated as below, $if(P + \dot{P}_{\text{storage}}) < P_{\text{demand}}$

$$\text{RP}_{\text{ES}}(\%) = \frac{|(P + \dot{P}_{\text{storage}}) - P_{\text{demand}}|}{(P + \dot{P}_{\text{storage}})} \times 100, \tag{24}$$

where,

$$\dot{P}_{\text{storage}} = P_{\text{storage}} - \Delta P_{\text{storage}} \tag{25}$$

denotes the new battery power due to loss of energy storage performance. As a consequence, any possible energy storage failure results in only derated state, which is illustrated in the state–space model shown in Fig. 8.

Other FCPP components such as reformer, stack, power conditioner and transformer are considered as essential components for the system power supply and the failure of any of these component can bring the system down. However, stack performance has gradual performance deterioration rather than catastrophic failures. As the electrodes and electrolyte become older, FCPP output voltage, and its power

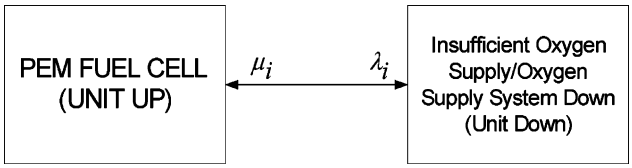

Fig. 7. The effect of oxygen supply system failure on FCPP based power generation in terms of state–space representation.

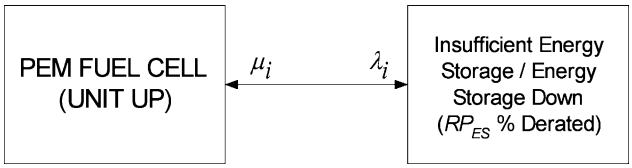

Fig. 8. The effect of energy storage failure on FC generation in terms of state–space representation.

Table 1
General format of the rules

Antecedent block: If input is [(weather conditions) and (load demand) and (. . .) and . . .]	Then	Consequent block: Output is [transition rates (failure rates, repair rates)]

drops steadily with time. Since this is more important for stand alone FCPPs, we did not consider this factor in this study.

3.2. Development of fuzzy Markov model (FMM)

In this paper, we performed the reliability analysis of grid using FMM, which is connected parallel to PEM FCPPs. Weather effects on failure and repair rates are incorporated in the grid outage model. In CMM based reliability analysis, it is assumed that transition rates, λ_{ij} are constant values. However, for power system reliability analysis, the transition rates varies from time to time depending on various factors such as weather conditions since the power system faults and their repair time are related to such conditions. Thus the relationship between input parameters (which can be weather temperature, load demand and power quality) and output parameters (such as failure and repair rates) can be mapped by fuzzy linguistic rules. The generalized structure of a FMM for n states is depicted in Fig. 9, and Table 1 shows its universe of discourse.

In Fig. 9, both failure rates and repair rates are represented by fuzzy membership functions [15], which are derived from the system outage statistics. The different system states are connected by fuzzy rules and the input variables to these rules can be weather conditions, or load demands, or both. For example, weather temperature is considered as an input variable, which represents climate conditions in fuzzy membership functions and may be different for different regions.

The number of antecedent variables in the universe of discourse can be increased or decreased by considering the available data based on both system configuration and region conditions. For instance, the universe of discourse given in Table 1 can be ruled as:

(1) "If the weather is stormy then failure rate and repair rate are high," or

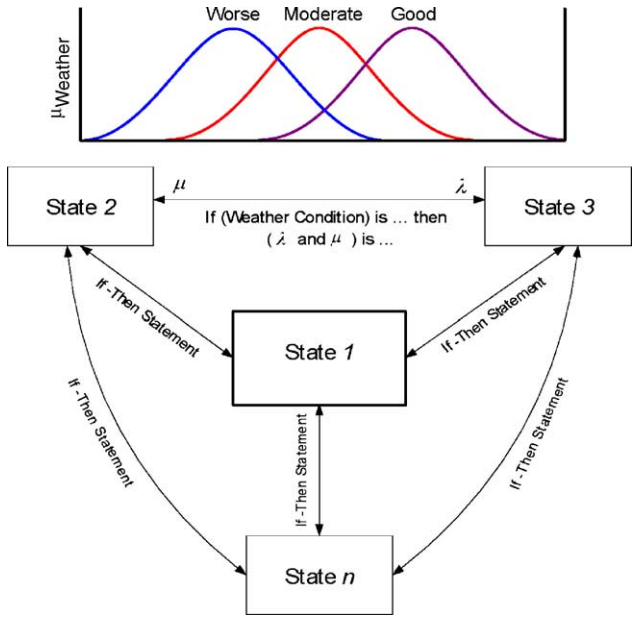

Fig. 9. Generalized structure of FMM for the reliability evaluation of grid load point.

(2) "If weather is stormy and temperature is very low then failure rate and repair rate are very high".

Due to the complexity of power systems, faults may not be catastrophic, and the operation of a power system can be graded from 0% to 100% by fuzzy numbers in the FMM. The transition rates in the FMM are related to several variables, such as, weather conditions, load demand, etc. The general representation of transition rates $\tilde{\lambda}_{ij}$ and the transition matrix, $\tilde{T}$ of the fuzzy Markov state–space diagram can be expressed as:

$$\tilde{\lambda}_{ij} = f(W_t, T_t, L_t) \tag{26}$$

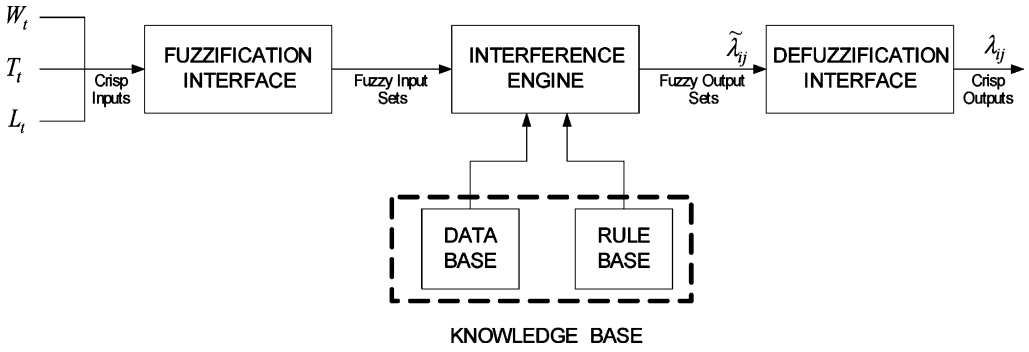

Fig. 10. The general fuzzy logic diagram for the developed FMM.

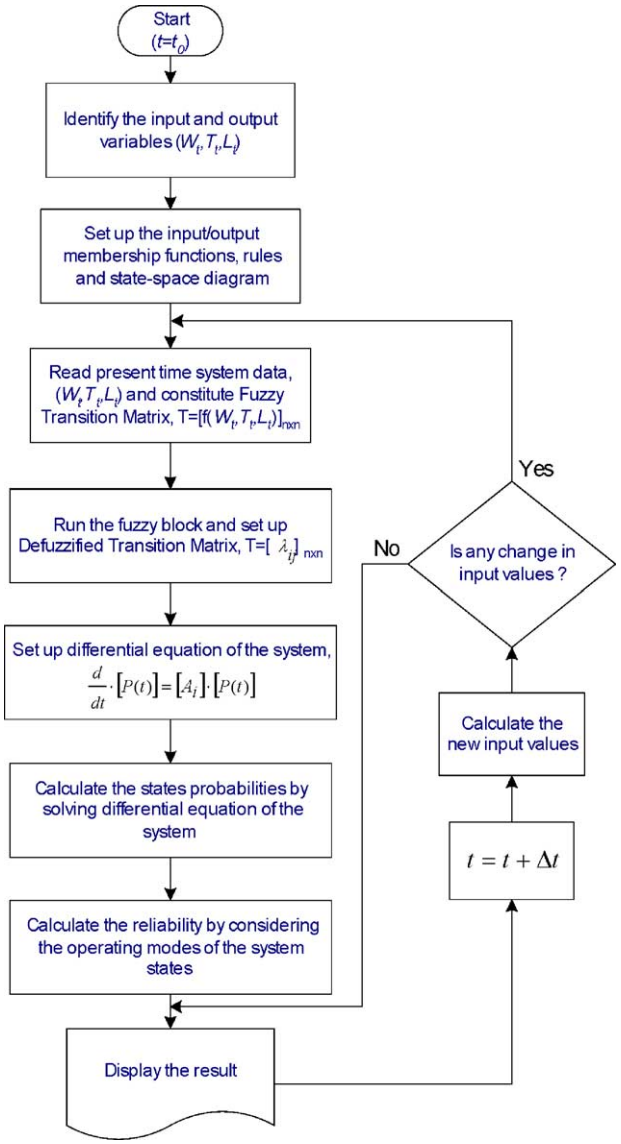

Fig. 11. The algorithm for the proposed FMM solution.

$$\tilde{T}=\begin{bmatrix} 0 & \tilde{\lambda}_{12}(W_t, T_t, L_t) & \cdots & \tilde{\lambda}_{1n}(W_t, T_t, L_t) \\ \tilde{\lambda}_{21}(W_t, T_t, L_t) & 0 & \cdots & \tilde{\lambda}_{2n}(W_t, T_t, L_t) \\ \cdots & \cdots & \cdots & \cdots \\ \tilde{\lambda}_{n1}(W_t, T_t, L_t) & \tilde{\lambda}_{n2}(W_t, T_t, L_t) & \cdots & 0 \end{bmatrix} \tag{27}$$

where t represents the sampling time, W represents the weather condition (windy, stormy, normal, etc.), T represents the weather temperature, L represents the load demand, and "$\sim$" represents the fuzzy relation. The relationship between λ_{ij} and W_t, T_t, L_t are connected by fuzzy linguistic rules as shown in Fig. 10. The corresponding FMM algorithm is shown in the flow chart of Fig. 11.

In Fig. 10, once the rules are established, a fuzzy logic system can be viewed as a mapping from inputs, W_t, T_i, and L_t to outputs, λ_{ij}. This mapping can be expressed quantitatively as $\lambda_{ij} = f(W_t, T_t, L_t)$. The max-min composition inference method is used in the inference engine block and the centroid method is used for defuzzification, defined as [16].

$$Z_C = \frac{\int_Z \mu_{C'}(z) z \cdot dz}{\int_Z \mu_{C'}(z) \cdot dz} \tag{28}$$

where $\mu_C(z)$ is the aggregated output membership function and Z_C is defuzzified system output.

The solution process of fuzzy Markov algorithm is as follows:

(1) define input variables and rules table,
(2) obtain the fuzzy transition matrix $\tilde{T}$ (Eq. (27)),
(3) defuzzification of Step 2 matrix, T, given as Eq. (29),

$$T = \begin{bmatrix} 0 & \lambda_{12} & \cdots & \lambda_{1n} \\ \lambda_{21} & 0 & \cdots & \lambda_{2n} \\ \cdots & \cdots & \cdots & \cdots \\ \lambda_{n1} & \lambda_{n2} & \cdots & 0 \end{bmatrix} \tag{29}$$

(4) Constitute state–space differential equation and obtain state probability by solving the state–space differential equation for inputs I_i. These steps are repeated for each new input value.

As for the FCPPs, assume that the failure rate of the auxiliary components increase with time until maintenance, and the failure rate drops to its original value after maintenance. It is also assumed that maintenance is performed at regular intervals, and the repair times and the duration of maintenance increase when the components grow older.

The relationship described in Fig. 12 is estimated by Weibull model, which is a practical tool for modeling component aging [17]. The Weibull distribution and its failure rate are defined as

$$f(T) = \frac{\beta T^{\beta-1}}{\alpha^\beta} \cdot e^{-(T/\alpha)^\beta} \tag{30}$$

$$\lambda(T) = \frac{\beta T^{\beta-1}}{\alpha^\beta} \tag{31}$$

where T is the component age (or time from last overhaul), β the shape factor which determines how the failure rate changes with equipment age (if $\beta < 1$ the failure rates decreases with age, if $\beta = 1$ the failure rate is independent of age, and if $\beta > 1$ the failure rate increases with age), and α is characteristic time interval. Since there is no publicly available data associated with the failures of FCPPs, a fuzzy logic rule base system is formed based on the expert knowledge to determine the performance loss of auxiliary components as illustrated in Table 2.

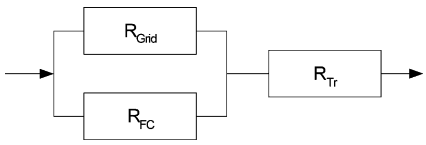

Fig. 12. Reliability model of grid-connected FC system.

Table 2
The general format of the rule for component state of health determination

Antecedent block: If input is [(component age) and (maintenance cycle) and (...)]	Then	Consequent block: Output is (state of health of component/degree of failure severity)

Once the individual FC and grid load point reliabilities are obtained, the results are combined using network representation technique for different operating time period with respect to weather conditions.

3.3. Reliability calculation

Normally, MM based system reliability is calculated by summing up all the operating state probabilities as shown below:

$$R = \sum_{i=1}^{n} P_i, \tag{32}$$

where P_i is a row vector and shows operating state probabilities. However, our concern is related to both up and derated states. If these state probabilities are grouped in the vector, then

$$P_i = [\, P_1^{\mathrm{u}} \quad P_2^{\mathrm{u}} \quad \cdots \quad P_m^{\mathrm{u}} \quad P_{m+1}^{\mathrm{d}} \quad P_{m+2}^{\mathrm{d}} \quad \cdots \quad P_n^{\mathrm{d}} \,]_{1\times n} \tag{33}$$

where "u" represent the up states and "d" represent the derated states. Derated state implies that the unit may not be able to develop full rated capacity. Thus, the derated state probabilities must be reduced by a reduction factor appropriate to the deratings. To take this effect into calculation, consider a correction vector, C_i, defined as

$$C_i = [\, 1 \quad 1 \quad \cdots \quad 1 \quad c_1 \quad c_2 \quad \cdots \quad c_n \,]^T_{1\times n} \tag{34}$$

where, $c_i = 1 - \mathrm{RP}_i^{\%}$ and $\mathrm{RP}_i^{\%}$ is the percent power reduction corresponding to each derated state.

Hence, the individual reliability of the system elements can be calculated as

$$R = [P_i]_{1\times n} \cdot [C_i]_{n\times 1} \tag{35}$$

Afterward, individual FCPP and grid reliabilities are combined to obtain the whole system reliability using network representation technique. Since this paper deals with grid-connected PEM FCPP that supplies a typical residential house through a transformer, the reliability model of the system can be depicted as shown in Fig. 12.

Combining the series and parallel connections, the system reliability can be calculated as

$$R_{\mathrm{sys}} = [1 - (1 - R_{\mathrm{Grid}}) \cdot (1 - R_{\mathrm{FC}})] \cdot R_{\mathrm{Tr}} \tag{36}$$

Consequently, the system reliability analysis throughout the operating time can be made by following the methodology repeatedly for multiple-weather conditions.

4. Example

In this study, an approach for reliability analysis of grid-connected PEM FCPPs is proposed. For illustration purposes,

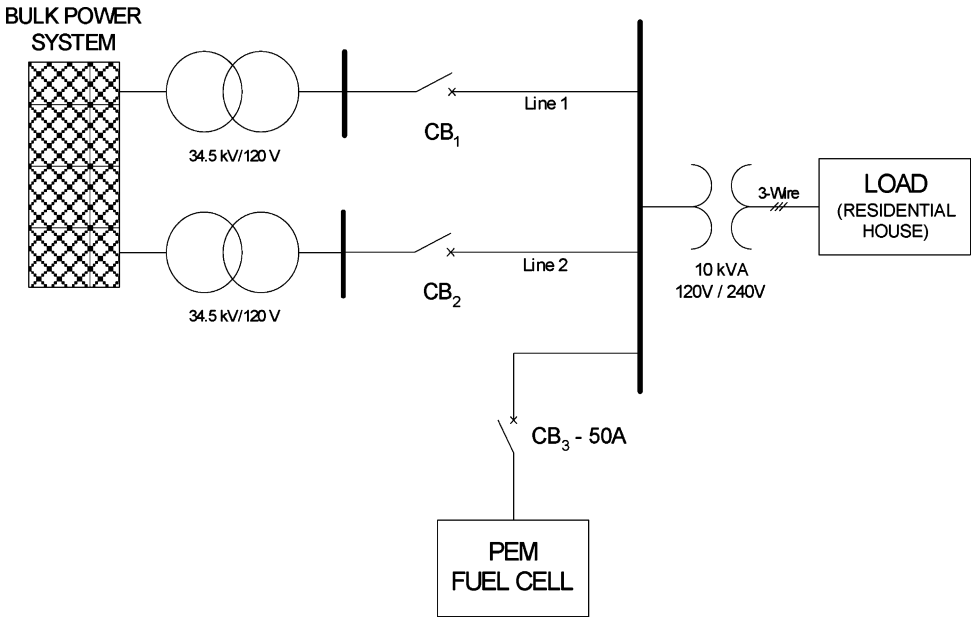

Fig. 13. Considered grid-connected PEM fuel cell system for reliability evaluation.

Table 3
A 5 kW PEM FCPP parameters

Parameter	Value	Parameter	Value
Cell Number	88	Oxygen partial pressure (atm)	2.17
Cell emf at STP (V)	0.6	Charge transfer constant	0.5
Universal gas constant (J mol^{-1} K^{-1})	8.1345	Stack current (A)	94.69
Stack temperature (K)	353	Limiting stack current (A)	105
Faraday's constant (C mol^{-1})	96485	Exchange current density (A cm^{-2})	$10^{-6.912}$
Hydr. partial pressure (atm)	1.087	Conc. voltage coefficient	0.0147
Water partial pressure (atm)	0.464	Stack internal resistance (Ohm)	0.00303

Table 4
Rule table for the functional relationship between input and output parameters

Antecedent block		Consequent block (% reductions in auxiliary performance)
If age is A_1 (very young)	Then	Reduction is B_1 (very healthy)
If age is A_2 (young)	Then	Reduction is B_2 (healthy)
If age is A_3 (medium)	Then	Reduction is B_3 (medium)
If age is A_4 (old)	Then	Reduction is B_4 (worn)
If age is A_5 (very old)	Then	Reduction is B_5 (very worn)

the proposed approach is applied to the system shown in Fig. 13.

A 5 kW Plug Power PEM FCPP installed at the University of South Alabama is considered in the sample system and the PEMFC parameters are given in Table 3. The proposed FCPP generation system model incorporates the input values (component age and maintenance cycle) and determines the degree of failure and failure rates via membership functions and Weibull distribution function. It is assumed that the possible wear out period starts after 5000 h of operation. The maintenance process is repeated at regular maintenance intervals. However, the repair time and the duration of maintenance increase at each cycle as the auxiliary components become older.

The input and output membership functions for an FCPP generation system modeling are depicted by the triangular membership function shown in Fig. 14. Since maintenance is done at regular intervals, component age gives direct information about the number of maintenance performed. Therefore, the input membership function is chosen only for component aging.

The rules used in the fuzzy inference system are listed in Table 4, which shows the functional relationship between component age and the reductions in auxiliary performance level.

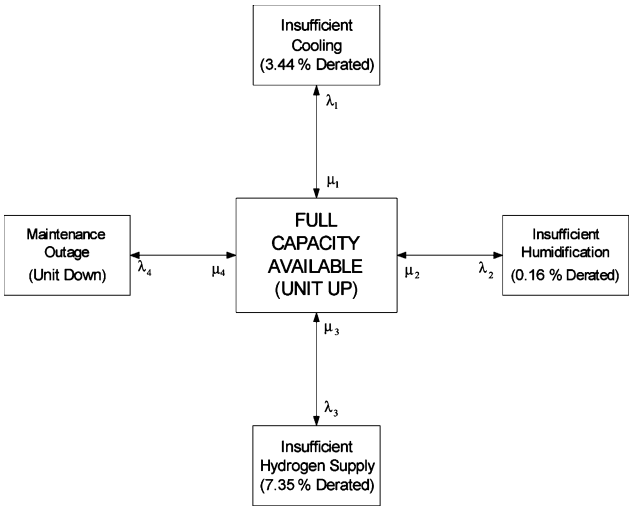

Fig. 15. The state–space model of a 5 kW PEMFC generating unit for 5th year operation, where $\lambda_1 = 1.1423 \times 10^{-4}$, $\lambda_2 = 1.1422 \times 10^{-4}$, $\lambda_3 = 1.1421 \times 10^{-4}$, $\lambda_4 = 1.1419 \times 10^{-4}$ (failure h^{-1}) and $\mu_1 = 0.3088$, $\mu_2 = 0.3388$, $\mu_3 = 0.3758$, $\mu_4 = 0.4$ (repair h^{-1}).

Fig. 15 shows the state–space model of a 5 kW PEM FCPP generation unit assuming 5 years of operation is established such that non-healthy states take place after a typical 5000-h operation time and maintenance is performed at 1-year regular intervals. After maintenance, it is assumed that the components become similar to a new one. In this model, battery backup is not taken into account since most grid-parallel PEM-FCPPs do not include any backup energy storage.

In Fig. 15, the performance loss for oxygen supply system is merged with full capacity available state since any reduc-

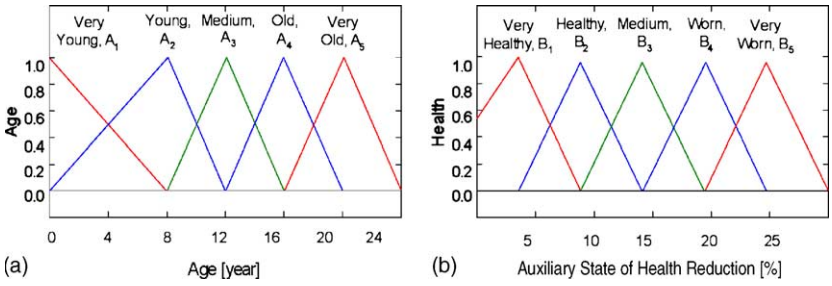

Fig. 14. Input (a) and output membership (b) functions for fuel cell generation system modeling.

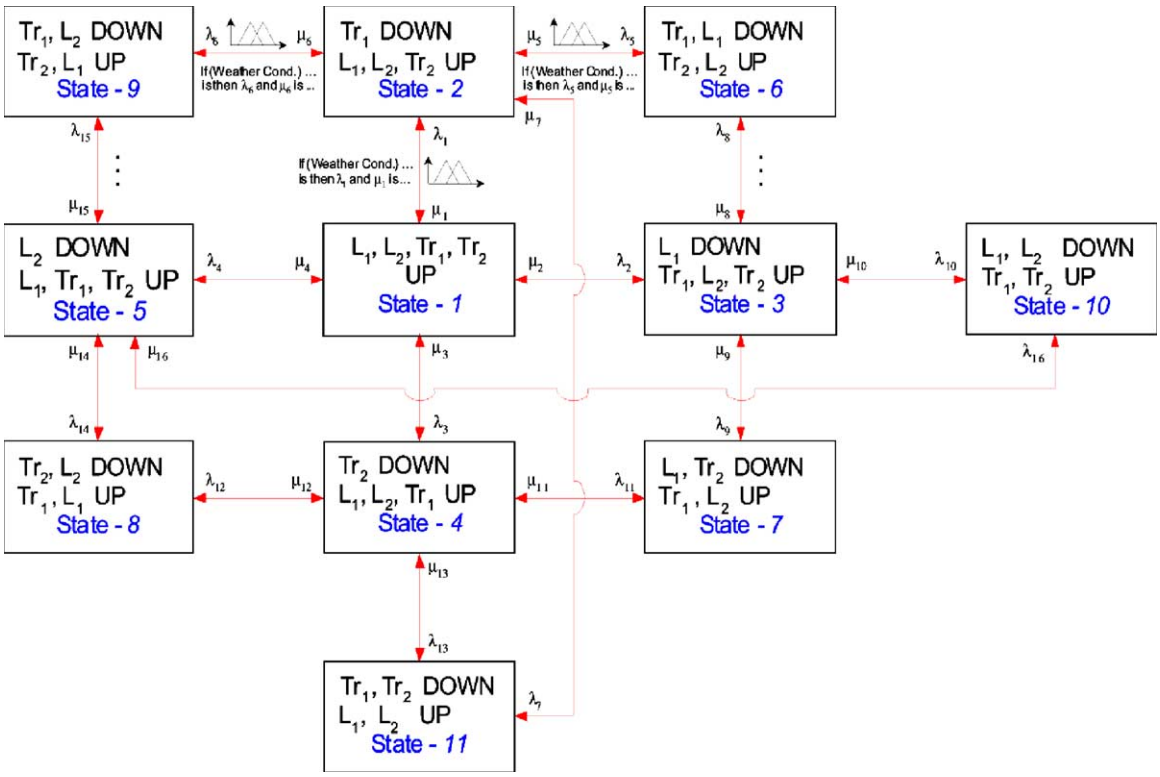

Fig. 16. Fuzzy Markov state–space diagram for the grid given in Fig. 13.

tion in oxygen supply does not lead to any derated/down state in a 5-year operation cycle. The transition probabilities in the model are estimated for each sub-system based on the Weibull distribution.

Fig. 16 shows eleven operating modes related to the state of load bus service, and outage data for a 1-year basis are listed in Table 5.

The input and output fuzzy variables of the FMM in the grid reliability study, temperature based seasonal membership functions, failure and repair rates, are derived by considering the past data and expert knowledge.

Here, the input is weather condition represented by temperatures based on four seasons. Since spring and autumn are very similar, judged by temperatures and other environmental conditions, they are combined. The outputs are the transition rates, namely failure and repair rates. The triangular membership functions are selected to model the transition rates for seasonal temperature, failure and repair rates as shown in Fig. 17.

The range of each output membership function was determined by the minimum and maximum transition rates, while the maximum membership point was determined by the transition rate considering the maximum number of occurrence in the period. The membership functions of failure rates are labeled as small (SM), medium (MED) and big (BIG). For the repair rates, the corresponding labels are little (LT), average (AVR) and high (HIG) as shown in Table 6. Some examples are shown in Fig. 17 (b) and (c) to illustrate the aforemen-

Table 5
The systems operation modes and its 1-year based outage data

Operating modes		Outage data	
Ref.	Failure of	Permanent outage (failure year^{-1})	Mean time to repair MTTR (h)
1. Grid up	No outage	–	–
2. Grid up	Tr_1	1.98	30
3. Grid up	$Line_1$	1.86	35
4. Grid up	Tr_2	2.04	35
5. Grid up	$Line_2$	1.86	42
6. Grid up	Tr_1, $line_1$	0.588	55
7. Grid down	$Line_1$, Tr_2	0.318	67
8. Grid up	Tr_2, $line_2$	0.594	65
9. Grid down	Tr_1, $line_2$	0.312	68
10. Grid down	$Line_1$, $line_2$	0.582	71
11. Grid down	Tr_1, Tr_2	0.612	70

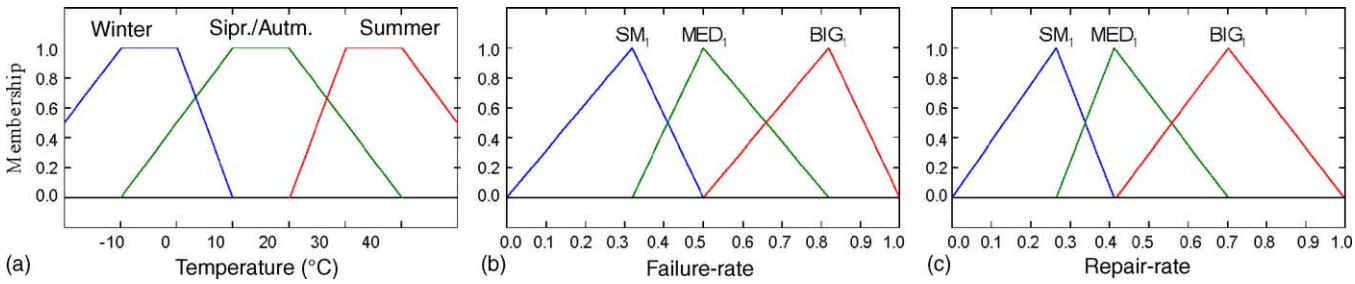

Fig. 17. Membership functions of (a) seasons based on temperature, (b) failure, and (c) repair rate.

Table 6
The linguistic rule table of FMM

Weather conditions	Fault and repair rates						
	λ_1	μ_1	λ_2	μ_2	...	λ_n	μ_n
Spr./aut.	MED_1	AVR_1					
Summer	SM_1	HIG_1					
Winter	BIG_1	LT_1					
Spr./aut.			MED_2	AVR_2			
Summer			SM_2	HIG_2			
Winter			BIG_2	LT_2			
...					...		
Spr./aut.						MED_n	AVR_n
Summer						SM_n	HIG_n
Winter						BIG_n	LT_n

tioned concept. The range of transition rates is scaled to the interval [0,1] by using different scaling factors for each output. The linguistic rules that connects the input and output variables are obtained for all possible transitions as shown in Table 6.

5. Simulation results

The simulation studies were conducted to investigate different aspects of the FCPP operation. The simulation of grid reliability variations using FMM is carried out for multiple weather conditions based on temperature, as shown in Fig. 18. While instantaneous grid reliability for –15, −5, 10, 25 and 35 °C weather conditions are shown respectively from the bottom to the top in Fig. 18 (a), reliability variation of the grid versus weather temperature is shown in Fig. 18 (b) by an increased number of temperature levels.

For testing the accuracy of the FMM approach, the state probabilities of the CMM and the FMM are compared at the 15 °C weather conditions, which can be assumed as a common point for both CMM and FMM. The results of this test, for each of the eleven operating modes, are given in Table 7. Although the accuracy of the results depends upon the accuracy of the models and system data, the correlation between the results of the two models is encouraging.

The simulation of FCPP reliability variations using the proposed approach is carried out for different lifetime of FCPP operation as shown in Fig. 19. While instantaneous FCPP reliability for 10-year operation period is given respectively from the bottom to the top in Fig. 19 (a), reliability variation of FCPP as a function of time (i.e., year) is shown in Fig. 19 (b).

Fig. 20 shows the entire system reliability variation versus weather temperature for different default value of transformer reliability and operational age, which is obtained by combining the FCPP, grid and transformer reliabilities. It is evident from Fig. 20 that the negative impact of weather temperature

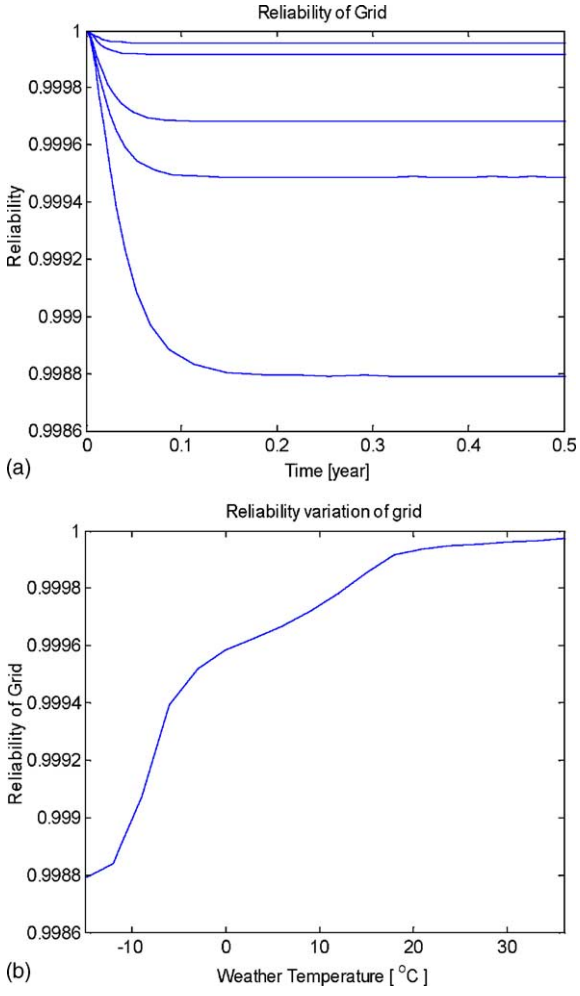

Fig. 18. Reliability variation of grid, (a) instantaneous grid reliability for −15, −5, 10, 25 and 35 °C weather conditions, and (b) reliability variation of the grid versus weather temperature.

Table 7
The comparison between the result of CMM and FMM for the 15 °C weather conditions of FMM

Operation states	The state probabilities	
	FMM solution	CMM solution
1	0.958764	0.959811
2	0.009297	0.009061
3	0.010184	0.009928
4	0.011168	0.010884
5	0.010250	0.009989
6	0.000051	0.000049
7	0.000037	0.000036
8	0.000067	0.000065
9	0.000034	0.000032
10	0.000068	0.000065
11	0.000079	0.000074

on grid reliability is almost vanished due to parallel connection of FCPP, and the negative impact of FCPP aging almost disappeared due to grid connection. At first glance, it seems that there is still considerable weather temperature and aging effect on system reliability. This is due to very short range

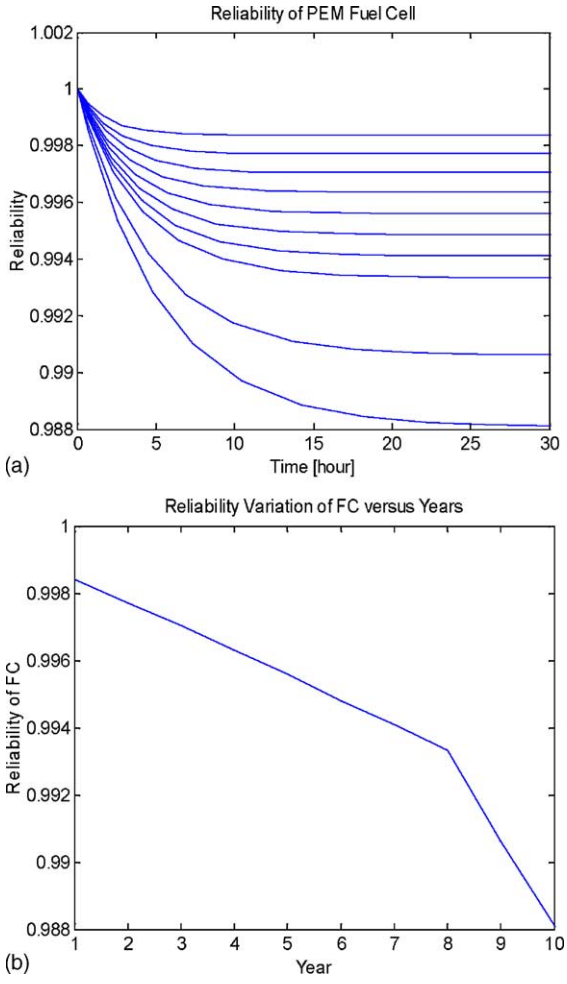

Fig. 19. Reliability variation of FC: (a) instantaneous FC reliability for 1, 2, . . ., 10 years (from upper to lower lines respectively), (b) reliability variation of the grid versus year.

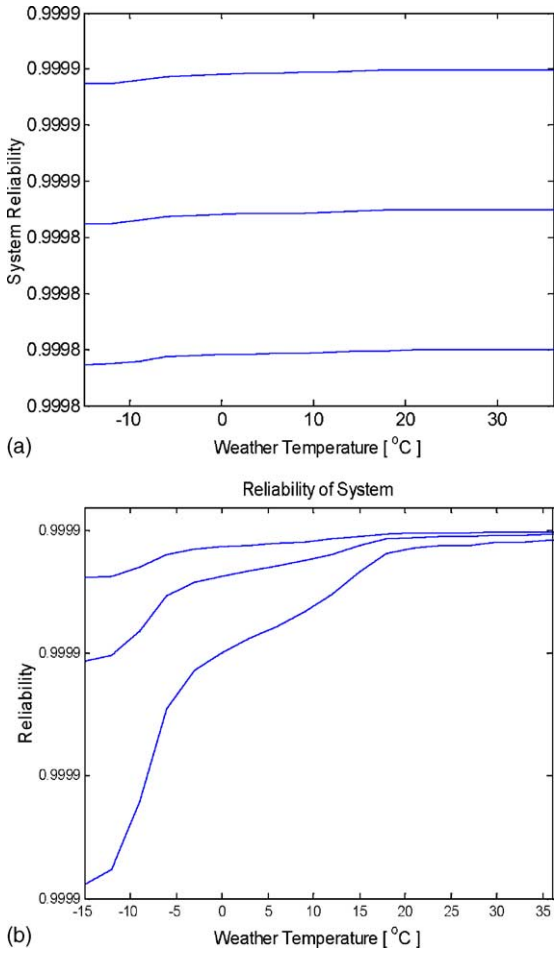

Fig. 20. Reliability variation of system versus weather temperature for: (a) transformer reliabilities of 0.9998, 0.99985, 0.9999 (respectively from bottom to top), (b) 1, 5 and 10 years of operation (respectively from top to bottom) in case transformer reliability is 0.9999.

of reliability (y axis) shown in Fig. 20 (a), and Fig. 20 (b), respectively. Indeed, the aforementioned effects on system reliability variation are very near to zero ($\sim 10^{-5}$).

If we consider the load bus reliability instead of the entire system, the availability of the bus would be 0.9999856 for the worst case scenario, and 0.999999952 for the best case scenario. This implies that the unavailability of load bus will be within the annual interruption time of 5 min to 3 s, which is an excellent service availability level.

6. Conclusions

In this paper, a new approach for reliability analysis of grid-connected PEM FCPP is developed based on the FMM. While the transition rates in FCPP state–space generation model is determined using Weibull distribution, fuzzy logic is used in the grid MM to describe both transition rates and temperature-based seasons (continuous-time, discrete-state FMM). The FMM is used to define the variation of grid reliability for multiple-weather conditions for different oper-

ational ages. The reliability of the entire system consists of parallel connection of grid and FCPP, which supplies load through a transformer, is obtained with respect to weather temperature and operational age of FCPP. The proposed method is an effective tool for reliability modeling of hybrid systems. Although this paper deals with grid-connected PEMFC power supply system, it gives a clear methodology for reliability modeling of stand alone FCPPs as well.

Although the transition rates are constant in the CMM, FMM can handle varying transition rates. If different weather conditions are to be handled by a CMM, the number of states in the model must increase in proportion to the number of weather conditions. However, the number of system states in the proposed FMM is constant for all weather conditions. The result of multiple weather calculation reveals that the major impact takes place during low temperature level. As for the aging effects on PEM-FCPP, FCPP reliability drops steadily with time as the components get older. However, in grid-connected system, the negative impacts of the aforementioned factors become negligible.

Acknowledgment

This work was supported in part by the U.S. Department of Energy (DE-FG02-02ER63376).

References

[1] J.E. Larmine, A. Dicks, Fuel Cell Systems Explained, John Wiley and Sons, Chichester, 2000.
[2] R. Billinton, E. Wojczynski, Distrubutional variation of distribution system reliability indices, IEEE Trans. Power Apparatus Syst. PAS-104 (11) (1985) 3152–3160.
[3] C. Singh, R. Billinton, System Reliability Modelling and Evaluation, Hutchison Educational, London, 1977.
[4] R. Billinton, A.V. Jain, Unit derating levels in spinning reserve studies. In: Proceedings of the 1971 IEEE Winter Power Meeting, Paper no. 71 T 120-PWR, 1971, p. 112.
[5] T.A.M. Sharaf, G.J. Berg, Loadability in composite generation/transmission power-system reliability evaluation, IEEE Trans. Reliability 42 (3) (1993) 393–400.
[6] R. Billinton, R.N. Allan, Reliability Evaluation of Engineering Systems: Concepts and Techniques, Plenum Press, London, 1983.
[7] R. Billinton, M.S. Grover, Reliabilty assesment of transmission and distribution schemes, IEEE Trans. Power Apparatus Syst. PAS-94 (3) (1975) 724–731.
[8] J.M. Cunningham, A.H. Myron, J.F. David, A Comparison of high-pressure and low-pressure operation of PEM fuel cell systems, in: Proceedings of SAE International, 2001, p. 538.
[9] S. Pischinger, C. Schönfelder, W. Bornscheuer, A.W. Kindl, Integrated air supply and humidification concepts for fuel cell systems, in: Proceedings of SAE International, 2001, p. 233.
[10] C.E. Thomas, Direct-Hydrogen-Fueled Proton-Exchange-Membrane Fuel Cell System for Transportation Applications, Ford Motor Company & U.S. Department of Energy Office of Transportation Technologies, 1997.
[11] J.T. Pukrushpan, A. Stefanopoulou, H. Peng, Modeling and control for PEM fuel cell stack system, in: Proceedings of the American Control Conference, 2002, pp. 3117–3122.
[12] D. Thirumalai, R.E. White, Mathematical modelling of proton-exchange-membrane fuel-cell stacks, J. Electrochem. Soc. 144 (1997) 1717–1723.
[13] F.N. Büchi, S. Srinivasan, Operation proton exchange membrane fuel cells without external humidification of the reactant gasses—fundamental aspects. J. Electrochem. Soc. (144) (8) 2767–2772.
[14] G. Sylvain, G. Anna, J. Stefanopoulou, T. Pukrushpan, P. Huei, Dynamics of low-pressure and high-pressure fuel cell air supply system, in: Proceedings of the American Control Conference, 2003.
[15] R. Kruse, R.B. Emden, R. Cordes, Processor power considerations an application of fuzzy Markov chains, Fuzzy Sets Syst. 21 (1985) 289–299.
[16] R.J. Jyh-Shing, S. Chuen-Tsai, Neuro-fuzzy modelling and control, in: Proceeding of the IEEE, vol. 83, issue 3, 1995, pp. 378–406.
[17] H.P. Barringer, K. Michael, Reliability of critical turbo/compressor equipment, in: Proceedings of the Fifth International Conference on Process Plant Reliability, 1996.